Interesting Directions in Flavor Physics

Alakabha Datta^{1,2,3}

¹Department of Physics and Astronomy, University of Mississippi, 108 Lewis Hall, Oxford, MS 38677, USA

²SLAC National Accelerator Laboratory, 2575 Sand Hill Road, Menlo Park, CA 94025, USA

³ Santa Cruz Institute for Particle Physics, Natural Sciences 2, Room 337 1156 High Street, Santa Cruz, CA 95064, USA

Abstract

Flavor physics continues to be an interesting avenue to look for beyond the standard model (SM) physics. Recent results from flavor physics, both in the quark and lepton sectors, hint at possible new physics. In this work we focus on some flavor physics results, mainly in b decays, and speculate on possible new physics interpretations of these results. We also present a model that can connect some of the B anomalies to the MiniBooNe anomaly and the muon g-2 measurement.

Keywords: symmetry, lepton, quarks, flavor physics

DOI: 10.31526/BSM-2023.1

1. INTRODUCTION

These are several interesting measurements in flavor experiments that could provide clues to BSM (beyond the SM) physics. Focussing, on the quark flavor sector, anomalies in the charged and neutral current B decays have been an active area of research for almost a decade. Although the updated measured values of $R_{K^{(*)}} = \mathcal{B}(B \to K^{(*)}\mu^+\mu^-)/\mathcal{B}(B \to K^{(*)}e^+e^-)$ are now fully consistent with the standard model (SM) expectations [1], the individual branching fractions remain lower than the SM predictions [2] which could indicate flavor universal new physics [3]. However, a first measurement by Belle II of the branching ratio $\mathcal{B}(B^+ \to K^+ \nu \bar{\nu}) = (2.3 \pm 0.7) \times 10^{-5}$ [4], which is 2.7σ higher than the SM expectation $\mathcal{B}(B^+ \to K^+ \nu \bar{\nu})_{\rm SM} = (5.58 \pm 0.38) \times 10^{-6}$ [5] has revived interest in neutral current B decays. For a limited list see [6, 7, 8, 9, 10, 11]; an earlier upper limit by Belle II [12] also led to a flurry of theoretical activity [13, 14, 15, 16, 17, 18]. Unlike the dilepton modes in $R_{K^{(*)}}$, the contamination from $c\bar{c}$ states in $B \to K^{(*)}\nu\bar{\nu}$ can be neglected. Hence, if confirmed, the Belle II result could be a clear sign of new physics.

On the other hand there are several puzzles in rare non leptonic B decays also and the most well known one is the so called $B \to \pi K$ puzzle which has ben discussed extensively in the literature. See for example [19] for a recent analysis of this puzzle. The $B \to \pi K$ puzzle can be considered to be part of a more general class of puzzles in hadronic B decays [20]. There are also several puzzles in the neutrino sector and it is a novel idea to explore a connection between the neutrino and the quark flavor anomalies.

In this work we will address a few of these anomalies. We will start with the anomalies in $b \to s$ transitions— $b \to s\ell^+\ell^-$, $b \to s\nu\bar{\nu}$.

2. $B \rightarrow K^{(*)}\ell^+\ell^-$ ANOMALY

The branching ratios for $B \to K^{(*)}\ell^+\ell^-$ and $B_s \to \phi\ell^+\ell^-$ are consistently below the SM predictions. As an illustration, consider the decays $B \to K\ell^+\ell^-$. In Figure 1, we show the experimental and theory calculations based on the lattice results [5] and one can see the deviations with respect to the SM predictions. A possible explanation of the anomalies is underestimated charm background but it is known for a long time that an universal new physics, ΔC_9 , can explain the data (see [3]). The amplitude for $B \to K^{(*)}\ell\bar{\ell}$ is

$$M_{\rm SM}\left(B \to K^{(*)}\ell\bar{\ell}\right) = -\frac{\alpha G_F}{\sqrt{2}\pi} V_{tb} V_{ts}^* \left[C_9 \left\langle K^{(*)} \left| \bar{s}_L \gamma^\mu b_L \right| B \right\rangle \bar{\ell} \gamma_\mu \ell + C_{10} \left\langle K^{(*)} \left| \bar{s}_L \gamma^\mu b_L \right| B \right\rangle \bar{\ell} \gamma_\mu \gamma^5 \ell \right]. \tag{1}$$

Moving over to $B \to K^{(*)} \nu \bar{\nu}$, the amplitude is

$$M_{\rm SM}\left(B \to K^{(*)} \nu \bar{\nu}\right) = -\frac{\alpha G_F}{\sqrt{2}\pi} V_{tb} V_{ts}^* C_L \left\langle K^{(*)} \left| \bar{s}_L \gamma^\mu b_L \right| B \right\rangle \bar{\nu} \gamma_\mu \left(1 - \gamma^5\right) \nu. \tag{2}$$

The key point is that the same form factor that is used in $B \to K^{(*)} \ell \bar{\ell}$ is applicable here.

As, indicated earlier the measured branching ratio for this decay is enhanced with respect to the SM prediction.

3. $B \rightarrow \pi K$ PUZZLE

We next move to puzzles in the hadronic decays. The set of $B \to \pi K$ decays are interesting because the amplitudes are related in the isospin limit which is an excellent symmetry for the strong interactions. The measured branching ratios and CP asymmetries for these decays, as shown in Table 1 [21] are difficult to understand in the SM.

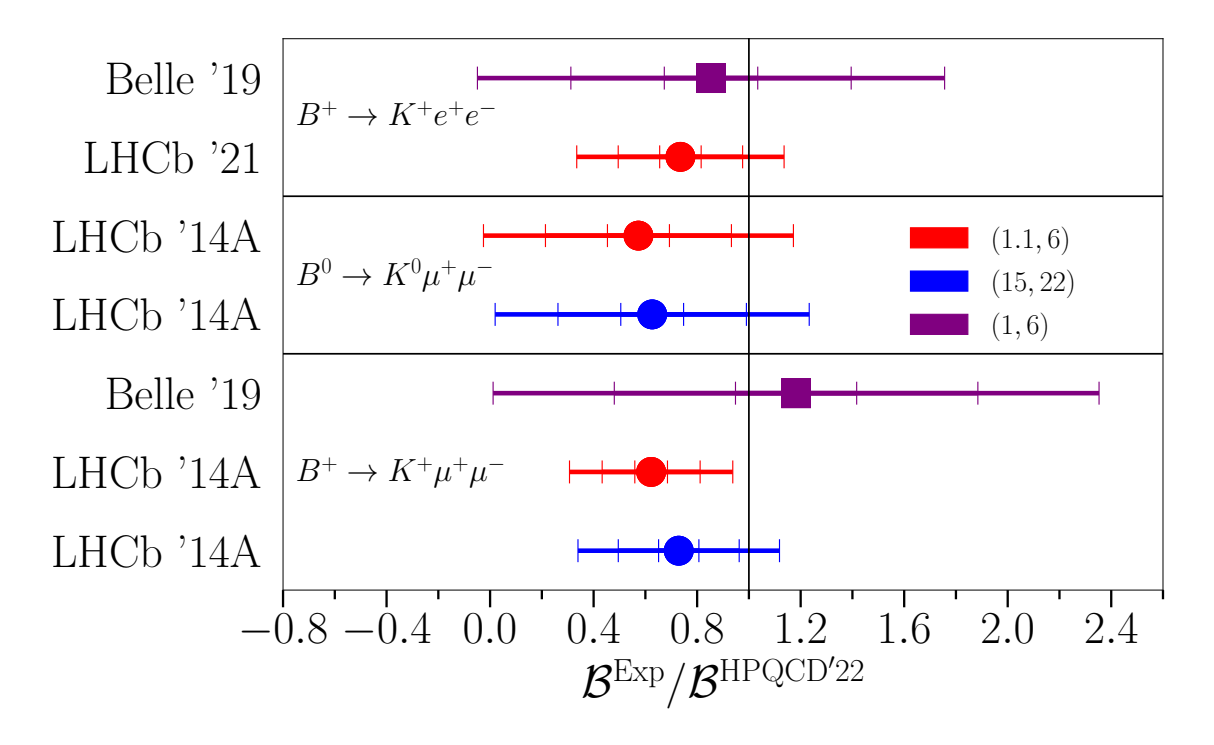


FIGURE 1: Branching ratios from experiment and theory for $B \to K\ell^+\ell^-$ [5].

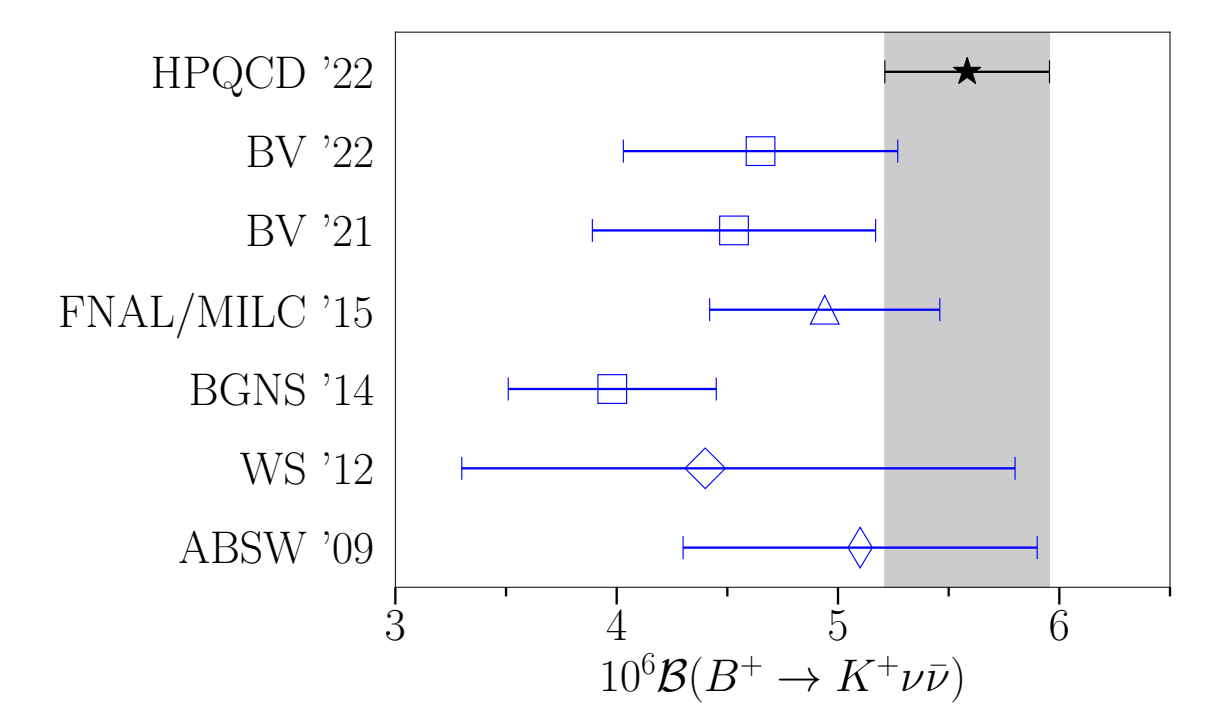


FIGURE 2: Branching ratios from theory for $B^+ \to K^+ \nu \bar{\nu}$ [5].

The leading order diagrams for the set of $B \to \pi K$ decays are shown in Figure 3.

Decay	$BR(\times 10^{-6})$	A_{CP}	S_{CP}
$B^+ o \pi^+ K^0$	23.79 ± 0.75	-0.017 ± 0.016	
$B^+ o \pi^0 K^+$	12.94 ± 0.52	0.025 ± 0.016	
$B_d^0 o \pi^- K^+$	19.57 ± 0.53	-0.084 ± 0.004	
$B_d^0 \to \pi^0 K^0$	9.93 ± 0.49	-0.01 ± 0.10	0.57 ± 0.17

TABLE 1: Branching ratios, direct CP asymmetries A_{CP} , and mixing-induced CP asymmetry S_{CP} (if applicable) for the four $B \to \pi K$ decay modes [21]. The A_{CP} measurements shown in red are predicted to be same in the SM in the leading order.

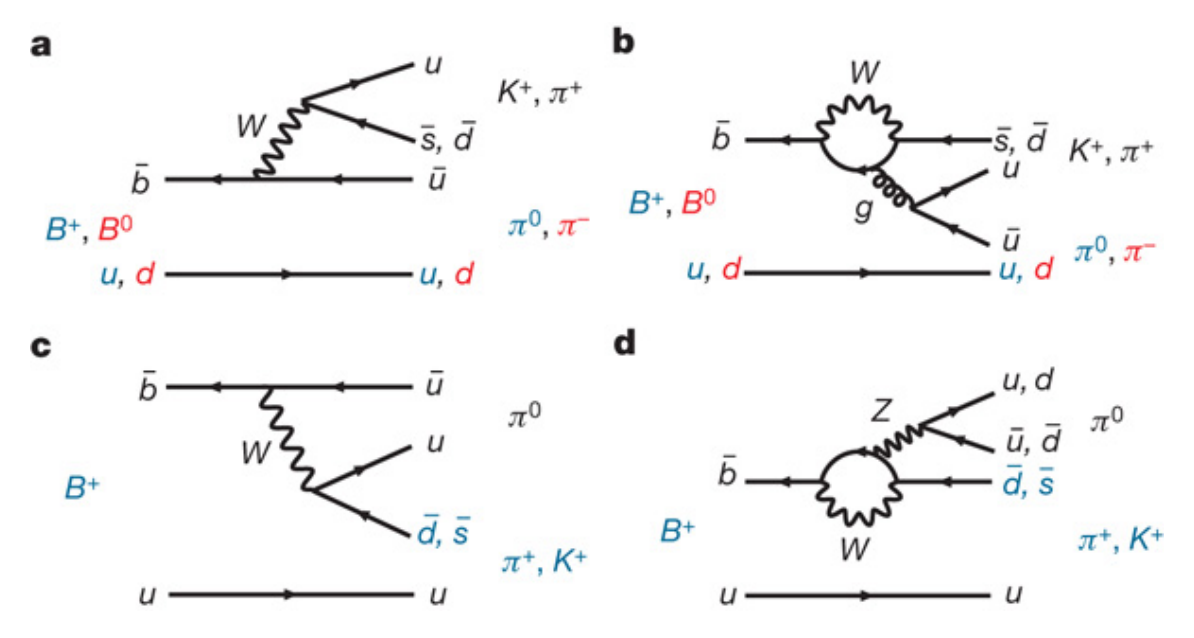


FIGURE 3: $B \rightarrow \pi K$ and $B \rightarrow \pi \pi$ diagrams.

We can describe all the $B \to \pi K$ decays by the following amplitudes: T', C', P', P'_{EW} , P'_{EW} which satisfy the following hierarchy.

$$\frac{|T'|}{|P'|} = \frac{|V_{ub}V_{us}|}{|V_{tb}V_{ts}|} \frac{C_1}{\frac{\alpha_s}{\pi}} \sim 0.15,\tag{3}$$

$$\frac{|C'|}{|P'|} = \frac{|C_2|}{|C_1|} \times \frac{|T'|}{|P'|} \sim 0.03,\tag{4}$$

$$\frac{|P'_{EW}|}{|P'|} = \frac{1.254\alpha}{\frac{\alpha_s}{2}} \sim 0.14,\tag{5}$$

$$\frac{|P_{EW}^{\prime C}|}{|P^{\prime}|} = \frac{|C_7|}{|C_9|} \times \frac{|P_{EW}^{\prime}|}{|P^{\prime}|} \sim 0..014. \tag{6}$$

This shows that these decays are penguin dominated and can be sensitive to new physics effects. On the other hand, the $B \to \pi\pi$ decays can be described by the following amplitudes: T, C, P, P_{EW} , P_{EW}^C . These decays are tree dominated and so less sensitive to new physics. The amplitudes satisfy

$$\frac{|P|}{|T|} = \frac{|V_{tb}V_{td}|}{|V_{ub}V_{ud}|} \frac{\frac{\alpha_s}{\pi}}{C_1} \sim 0.10,\tag{7}$$

$$\frac{|C|}{|T|} = \frac{|C_2|}{|C_1|} \sim 0.,\tag{8}$$

$$\frac{|P_{EW}|}{|P|} = \frac{1.254\alpha}{\frac{\alpha_s}{\pi}} \sim 0.14,\tag{9}$$

$$\frac{|P_{EW}^{c}|}{|P|} = \frac{|C_{7}|}{|C_{9}|} \times \frac{|P_{EW}|}{|P|} \sim 0 \cdots 014. \tag{10}$$

For the $A^{ij} \equiv B \rightarrow \pi^i K^j$ amplitudes, one can write after dropping small amplitudes:

$$A^{+0} = -P'_{tc} + P'_{uc}e^{i\gamma} - \frac{1}{3}P'^{C}_{EW}, \tag{11}$$

$$\sqrt{2}A^{0+} = -T'e^{i\gamma} - C'e^{i\gamma} + P'_{tc} - P'_{uc}e^{i\gamma} - P'_{EW} - \frac{2}{3}P'^{C}_{EW},$$
(12)

$$A^{-+} = -T'e^{i\gamma} + P'_{tc} - P'_{uc}e^{i\gamma} - \frac{2}{3}P'^{C}_{EW}, \tag{13}$$

$$\sqrt{2}A^{00} = -C'e^{i\gamma} - P'_{tc} + P'_{uc}e^{i\gamma} - P'_{EW} - \frac{1}{3}P'^{C}_{EW}.$$
(14)

The electroweak amplitudes are related by the Tree amplitudes in the SU(3) limit via

$$P'_{EW} = \frac{3}{4} \frac{c_9 + c_{10}}{c_1 + c_2} R(T' + C') + \frac{3}{4} \frac{c_9 - c_{10}}{c_1 - c_2} R(T' - C'),$$

$$P'_{EW} = \frac{3}{4} \frac{c_9 + c_{10}}{c_1 + c_2} R(T' + C') - \frac{3}{4} \frac{c_9 - c_{10}}{c_1 - c_2} R(T' - C').$$
(15)

At fit to the data is shown in Table 1 gives the following result in Table 2.

χ^2/dof	3.18/2	
Parameter	Fitted Value	
$ P'_{tc} $	50.7 ± 1.7	
T'	5.5 ± 1.5	
C'	3.8 ± 1.3	
$ P'_{uc} $	1.0 ± 9.1	
$\delta_{P'_{tc}}$	-16.0 ± 7.3	
$\delta_{C'}$	205 ± 20	
$\delta_{P'_{uc}}$	8.0 ± 350	

TABLE 2: All SM parameters all data.

We can make the following observation from Table 2:

- (i) |C'/T'| = 0.68 is pretty large and is generally inconsistent with observations from color suppressed decays.
- (ii) The default expectation $|C'/T'| \sim 0.2$ (see, e.g., QCD factorization) will worsen the fit.
- (iii) ACP(00) = -0.11 while the central value of the measurement is -0.01 with a large uncertainty. Hence precise measurement of the CP asymmetry in $B_d^0 \to \pi^0 K^0$ is crucial.

Using the expected value of |C'/T'| = 0.2 we get a poor fit to the data as shown in Table 3.

χ^2/dof	26.7/5
Parameter	Fitted Value
$ P'_{tc} $	46.23 ± 0.50
T'	5.33 ± 0.72
$\delta_{P'_{tc}}$	-23.5 ± 3.9
$\delta_{C'}^{ii}$	220 ± 16

TABLE 3: $P'_{uc} = 0$, |C'/T'| = 0.2, all data.

4. EFFECTIVE OPERATORS: SMEFT

One can explore whether in SMEFT (standard model effective field theory) one can explain the semi leptonic and hadronic puzzles from a common set of operators as shown in Table 4 using qcd and electroweak RGE running.

$Q_{qq}^{(1)}$	$(\bar{q}_i\gamma_\mu q_j)(\bar{q}_k\gamma^\mu q_\ell)$	$(\bar{L}L)(\bar{L}L)$	qq1_2333
$Q_{qq}^{(3)}$	$(ar{q}_i \gamma_\mu au^I q_j) (ar{q}_k \gamma^\mu au^I q_\ell)$	(LL)(LL)	qq3_2333
$Q_{qd}^{(1)}$	$(ar{q}_i \gamma_\mu q_j)(ar{d}_k \gamma^\mu d_\ell)$	(<u>L</u> L)(<u>R</u> R)	qd1_2333
$Q_{qd}^{(8)}$	$(\bar{q}_i\gamma_\mu T^Aq_i)(\bar{d}_k\gamma^\mu T^Ad_\ell)$	(22)(111)	qd8_2333
Q_{dd}	$(\bar{d}_i\gamma_\mu d_j)(\bar{d}_k\gamma^\mu d_\ell)$	$(\bar{R}R)(\bar{R}R)$	dd_2333

TABLE 4: SMEFT operators.

At the m_b scale, from the SMEFT operators in Table 4, we can generate both $b \to sq\bar{q}$ and $b \to s\ell^+\ell^-$ operators. The operators relavant for non leptonic decays are

$$C_{V_{LL}}^{q} \frac{4G_F}{\sqrt{2}} V_{tb} V_{ts}^* \left(\bar{s}_L \gamma_\mu b_L\right) \left(\bar{q}_L \gamma^\mu q_L\right), \quad C_{V_{LR}}^{q} \frac{4G_F}{\sqrt{2}} V_{tb} V_{ts}^* \left(\bar{s}_L \gamma_\mu b_L\right) \left(\bar{q}_R \gamma^\mu q_R\right), \tag{16}$$

$$C_{V_{RL}}^{q} \frac{4G_F}{\sqrt{2}} V_{tb} V_{ts}^* \left(\bar{s}_R \gamma_\mu b_R\right) \left(\bar{q}_L \gamma^\mu q_L\right), \quad C_{V_{RR}}^{q} \frac{4G_F}{\sqrt{2}} V_{tb} V_{ts}^* \left(\bar{s}_R \gamma_\mu b_R\right) \left(\bar{q}_R \gamma^\mu q_R\right), \tag{17}$$

$$C_{V_{LL}}^{q,C} \frac{4G_F}{\sqrt{2}} V_{tb} V_{ts}^* \left(\bar{s}_L^{\alpha} \gamma_{\mu} b_L^{\beta} \right) \left(\bar{q}_L^{\beta} \gamma^{\mu} q_L^{\alpha} \right), \quad C_{V_{LR}}^{q,C} \frac{4G_F}{\sqrt{2}} V_{tb} V_{ts}^* \left(\bar{s}_L^{\alpha} \gamma_{\mu} b_L^{\beta} \right) \left(\bar{q}_R^{\beta} \gamma^{\mu} q_R^{\alpha} \right), \tag{18}$$

$$C_{V_{RL}}^{q,\mathcal{C}} \frac{4G_F}{\sqrt{2}} V_{tb} V_{ts}^* \left(\bar{s}_R^{\alpha} \gamma_{\mu} b_R^{\beta} \right) \left(\bar{q}_L^{\beta} \gamma^{\mu} q_L^{\alpha} \right), \quad C_{V_{RR}}^{q,\mathcal{C}} \frac{4G_F}{\sqrt{2}} V_{tb} V_{ts}^* \left(\bar{s}_R^{\alpha} \gamma_{\mu} b_R^{\beta} \right) \left(\bar{q}_R^{\beta} \gamma^{\mu} q_R^{\alpha} \right). \tag{19}$$

On the other hand, the semileptonic operator is

$$C_9^{bs\ell\ell} \frac{4G_F}{\sqrt{2}} V_{tb} V_{ts}^* \frac{e^2}{16\pi^2} \left(\bar{s}_L \gamma_\mu b_L \right) \left(\bar{\ell} \gamma^\mu \ell \right). \tag{20}$$

Hence, four quark SMEFT operators can potentially explain both the $b \to s\ell^+\ell^-$ and $b \to sq\bar{q}$ anomalies. Strong constraints in these models come from B_s mixing.

5. $B \rightarrow K \nu \bar{\nu}$ AND THE MINIBOONE ANOMALY

An interesting possibility is to explore a link between anomalies in B decays to neutrino and anomalies in neutrino experiments. In this section we explore a model of a light scalar mixing with an extended Higgs sector to explain the $B \to K \nu \bar{\nu}$ and the MiniBooNE anomalies. The MiniBooNE anomaly is characterized by excess electron-like events in the energy region between 200 MeV and 600 MeV and is coincident in time with the $\langle E_{\nu} \rangle \sim 0.8$ GeV neutrino beam. It is now considered a 4.8σ significance effect. The Lagrangian of our model is [22]

$$\mathcal{L}_{S} \supset \frac{1}{2} \left(\partial_{\mu} S \right)^{2} - \frac{1}{2} m_{S}^{2} S^{2} - \eta_{d} \sum_{f=d,\ell} \frac{m_{f}}{v} \bar{f} f S - \sum_{f=u,c,t} \eta_{f} \frac{m_{f}}{v} \bar{f} f S - g_{D} S \bar{\nu}_{D} \nu_{D} - \frac{1}{4} \kappa S F_{\mu\nu} F^{\mu\nu},$$
(21)

where $v \simeq 246\,\text{GeV}$, is the Higgs vacuum expectation value, d and ℓ correspond to down-type quarks and leptons with a universal coupling η_d scaled by the respective SM Yukawa. The structure of the Lagrangian can arise from the mixing of singlet scalar with the neutral components of a two Higgs doublet model [23, 24, 25]. We will however adopt an effective interaction in the spirit of [26] and take the couplings η_f of the scalar to the up-type quarks to not be flavor universal. The FCNC $B \to KS$ and $K \to \pi S$ decays are generated by the penguin diagrams in Figure 4

$$\mathcal{L}_{\text{FCNC}} = g_{bs}\bar{s}P_RbS + g_{sd}\bar{d}P_RsS,\tag{22}$$

$$g_{bs} \approx \frac{3\sqrt{2}G_F}{16\pi^2} \frac{m_t^2 m_b}{v} \eta_t V_{tb} V_{ts}^*,$$
 (23)

$$g_{sd} \approx \frac{3\sqrt{2}G_F}{16\pi^2} \frac{m_t^2 m_s}{v} V_{ts} V_{td}^* \left(\eta_t + \eta_c \frac{m_c^2}{m_t^2} \frac{V_{cs} V_{cd}^*}{V_{ts} V_{td}^*} \right). \tag{24}$$

The MiniBooNE events are generated in the model via neutrino scattering in Figures 5 and 6. The predictions of the model for certain benchmark points are shown in Table 5.

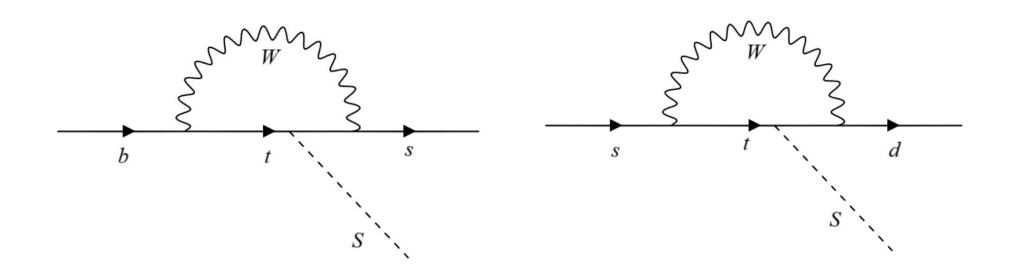


FIGURE 4: Penguin diagrams for $b \to s\phi$ and $s \to d\phi$.

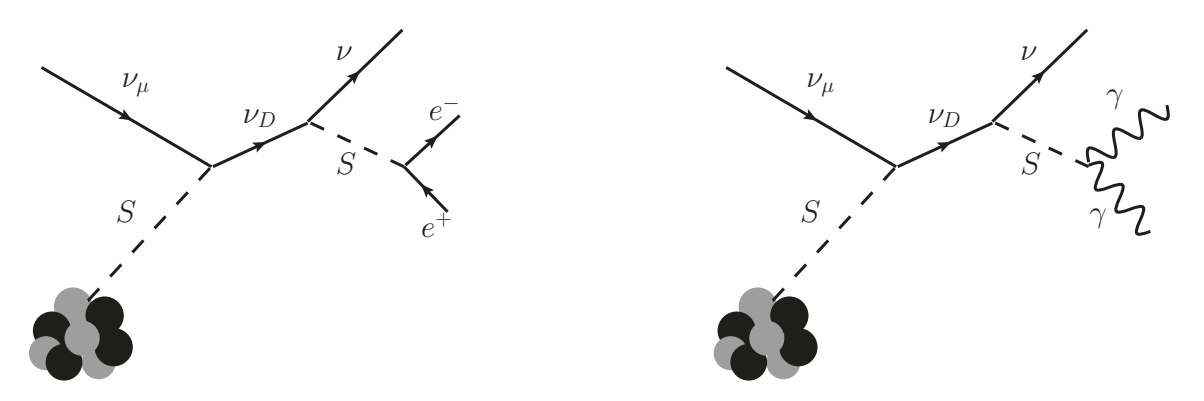


FIGURE 5: MiniBooNe neutrino interaction with $S \rightarrow e^+e^-$.

FIGURE 6: MiniBooNe neutrino interaction with $S \to \gamma \gamma$.

BP	$\mathcal{B}(S o\gamma\gamma)$	$\mathcal{B}(S \to \nu \bar{\nu})$	$\mathcal{B}(S \to e^+e^-)$	$\mathcal{B}(K_L \to \pi^0 \nu \bar{\nu})$	$\mathcal{B}(B_s \to \nu \bar{\nu})$	$\mathcal{B}(B \to K^{(*)}\gamma\gamma)$
1	0.093	0.907	4.26×10^{-5}	1.71×10^{-9}	5.13×10^{-7}	1.3×10^{-6}
2	0.717	0.282	7.06×10^{-4}	3.61×10^{-11}	3.54×10^{-7}	3.7×10^{-5}
3	0.496	0.504	5.93×10^{-5}	9.02×10^{-10}	4.14×10^{-7}	1.7×10^{-5}
4	0.165	0.835	1.10×10^{-4}	1.73×10^{-9}	1.43×10^{-6}	2.65×10^{-6}
5	0.829	0.170	9.72×10^{-4}	2.04×10^{-10}	1.72×10^{-7}	6.8×10^{-5}
6	4.58×10^{-6}	0.999	7.10×10^{-4}	1.89×10^{-9}	1.01×10^{-6}	6.5×10^{-11}
7	3.95×10^{-4}	0.997	2.14×10^{-3}	2.84×10^{-9}	4.86×10^{-7}	7.6×10^{-9}

TABLE 5: Predictions for certain benchmark points of the model [22].

5.1. Predictions—S Model

The main predictions of the model are the following:

- (i) $K_L \rightarrow \pi^0$ + inv can be close to the experimental bound.
- (ii) A resonance in $B \to K^{(*)} \gamma \gamma$ is the main prediction.
- (iii) The branching ratio of S to electron-positron pair is tiny and so $b \to s\ell^+\ell^-(B \to K^{(*)}\ell^+\ell^-)$ decays is mostly SM.

5.2. a_{μ} , a_e Constraints/Predictions

The model can explain the muon g-2 measurement [27] also via the diagrams in Figure 7. Because of small S coupling to leptons the Barr-Zee diagram dominates.

$$\delta(g-2)_{\ell}^{S\gamma\gamma} \approx \frac{\eta_d}{4\pi^2} \frac{\kappa m_{\ell}^2}{v} \ln \frac{\Lambda}{m_S}.$$
 (25)

Note that η_d and κ control the $S \to e^+e^-$ and $S \to \gamma\gamma$ rates.

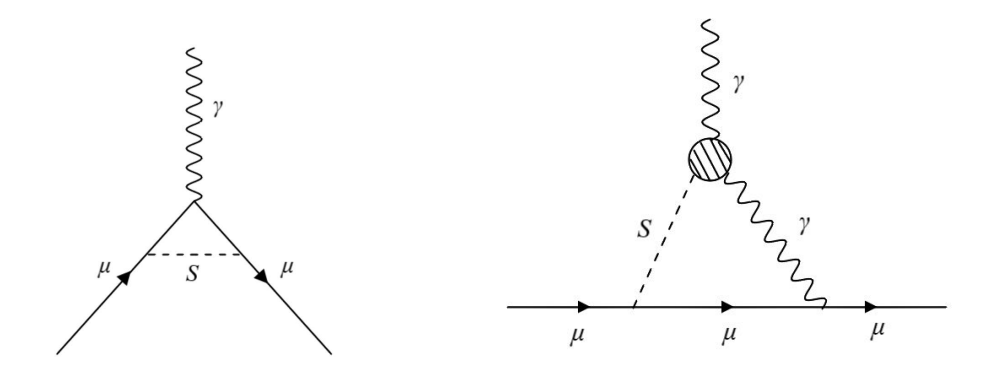


FIGURE 7: The scalar *S* contributions to $(g-2)_u$.

6. SUMMARY

In summary there are several puzzles in $b \to s$ transitions in semileptonic and nonleptonic B decays. A unified description may be possible in an effective theory through RGE effects of SMEFT operators. There is new evidence for $B^+ \to K^+ + inv$ with an enhanced rate relative to the SM. We considered a model where this decay is interpreted as $B^+ \to K^+ + S$, where S is a short lived scalar that decays to neutrinos by coupling to a sterile neutrino v_4 , which mixes with the muon light neutrino. The same model can provide an explanation of the MiniBooNE electron like events events as well as the muon g-2 measurement.

ACKNOWLEDGMENTS

Alakabha Datta thanks the SLAC National Accelerator Laboratory and the Santa Cruz Institute of Particle Physics for their hospitality during the completion of this work. Alakabha Datta is supported in part by the U.S. National Science Foundation under Grant No. PHY-2309937 D.M. is supported in part by the U.S. Department of Energy under Grant No. de-sc0010504.

References

- [1] R. Aaij et al. [LHCb], "Test of lepton universality in $b \to s\ell^+\ell^-$ decays," Phys. Rev. Lett. **131**, no.5, 051803 (2023) doi:10.1103/PhysRevLett.131.051803 [arXiv:2212.09152 [hep-ex]].
- [2] B. Capdevila, A. Crivellin, and J. Matias, "Review of Semileptonic *B* Anomalies," Eur. Phys. J. ST **1**, 20 (2023) doi:10.1140/epjs/s11734-023-01012-2 [arXiv:2309.01311 [hep-ph]].
- [3] A. Datta, M. Duraisamy, and D. Ghosh, "Explaining the $B \to K^* \mu^+ \mu^-$ data with scalar interactions," Phys. Rev. D 89, no.7, 071501 (2014) doi:10.1103/PhysRevD.89.071501 [arXiv:1310.1937 [hep-ph]].
- [4] I. Adachi et al. [Belle-II], "Evidence for $B^+ \to K^+ \nu \bar{\nu}$ Decays," [arXiv:2311.14647 [hep-ex]].
- [5] W. G. Parrott et al. [HPQCD], "Standard Model predictions for $B \rightarrow K\ell + \ell -$, $B \rightarrow K\ell + \ell -$ and $B \rightarrow K\nu\nu^-$ using form factors from Nf = 2 + 1 + 1 lattice QCD," Phys. Rev. D **107**, no.1, 014511 (2023) [erratum: Phys. Rev. D **107**, no.11, 119903 (2023)] doi:10.1103/PhysRevD.107.014511 [arXiv:2207.13371 [hep-ph]].
- [6] R. Bause, H. Gisbert, and G. Hiller, "Implications of an enhanced $B \rightarrow K \nu \nu^-$ branching ratio," Phys. Rev. D **109**, no.1, 015006 (2024) doi:10.1103/PhysRevD.109.015006 [arXiv:2309.00075 [hep-ph]].
- [7] L. Allwicher, D. Becirevic, G. Piazza, S. Rosauro-Alcaraz, and O. Sumensari, "Understanding the first measurement of $B(B \rightarrow K\nu\nu^-)$," Phys. Lett. B **848**, 138411 (2024) doi:10.1016/j.physletb.2023.138411 [arXiv:2309.02246 [hep-ph]].
- [8] P. Athron, R. Martinez, and C. Sierra, "B meson anomalies and large $B^+ \to K^+ \nu \overline{\nu}$ in non-universal $U(1)^?$ models," JHEP **02**, 121 (2024) doi:10.1007/JHEP02(2024)121 [arXiv:2308.13426 [hep-ph]].
- [9] T. Felkl, A. Giri, R. Mohanta, and M. A. Schmidt, "When energy goes missing: new physics in $b \rightarrow s\nu\nu$ with sterile neutrinos," Eur. Phys. J. C 83, no.12, 1135 (2023) doi:10.1140/epjc/s10052-023-12326-9 [arXiv:2309.02940 [hep-ph]].
- [10] X. G. He, X. D. Ma, and G. Valencia, "Revisiting models that enhance $B^+ \to K^+ \nu \bar{\nu}$ in light of the new Belle II measurement," [arXiv:2309.12741 [hep-ph]].
- [11] C. H. Chen and C. W. Chiang, "Flavor anomalies in leptoquark model with gauged $U(1)_{L_{\mu}-L_{\tau}}$," [arXiv:2309.12904 [hep-ph]].
- [12] F. Abudinén et al. [Belle-II], "Search for $B+\rightarrow K+\nu\nu$ " Decays Using an Inclusive Tagging Method at Belle II," Phys. Rev. Lett. 127, no.18, 181802 (2021) doi:10.1103/PhysRevLett.127.181802 [arXiv:2104.12624 [hep-ex]].
- [13] T. E. Browder, N. G. Deshpande, R. Mandal, and R. Sinha, "Impact of $B \rightarrow K\nu\nu^-$ measurements on beyond the Standard Model theories," Phys. Rev. D **104**, no.5, 053007 (2021) doi:10.1103/PhysRevD.104.053007 [arXiv:2107.01080 [hep-ph]].
- [14] X. G. He and G. Valencia, "*RK*(*)ν and non-standard neutrino interactions," Phys. Lett. B **821**, 136607 (2021) doi:10.1016/j.physletb.2021.136607 [arXiv:2108.05033 [hep-ph]].
- [15] T. Felkl, S. L. Li, and M. A. Schmidt, "A tale of invisibility: constraints on new physics in $b \rightarrow s\nu\nu$," JHEP 12, 118 (2021) doi:10.1007/JHEP12(2021)118 [arXiv:2111.04327 [hep-ph]].
- [16] X. G. He, X. D. Ma, and G. Valencia, "FCNC B and K meson decays with light bosonic Dark Matter," JHEP 03, 037 (2023) doi:10.1007/JHEP03(2023)037 [arXiv:2209.05223 [hep-ph]].

[17] M. Ovchynnikov, M. A. Schmidt, and T. Schwetz, "Complementarity of $B \to K^{(*)} \mu \bar{\mu}$ and $B \to K^{(*)} + inv$ for searches of GeV-scale Higgs-like scalars," Eur. Phys. J. C 83, no.9, 791 (2023) doi:10.1140/epjc/s10052-023-11975-0 [arXiv:2306.09508 [hep-ph]].

- [18] P. Asadi, A. Bhattacharya, K. Fraser, S. Homiller, and A. Parikh, "Wrinkles in the Froggatt-Nielsen mechanism and flavorful new physics," JHEP 10, 069 (2023) doi:10.1007/JHEP10(2023)069 [arXiv:2308.01340 [hep-ph]].
- [19] N. B. Beaudry, A. Datta, D. London, A. Rashed, and J. S. Roux, "The $B \to \pi K$ puzzle revisited," JHEP **01**, 074 (2018) doi:10.1007/JHEP01(2018)074 [arXiv:1709.07142 [hep-ph]].
- [20] R. Berthiaume, B. Bhattacharya, R. Boumris, A. Jean, S. Kumbhakar, and D. London, "Anomalies in Hadronic *B* Decays," [arXiv:2311.18011 [hep-ph]].
- [21] Y. S. Amhis et al. [HFLAV], "Averages of *b*-hadron, *c*-hadron, and τ-lepton properties as of 2021," Phys. Rev. D **107**, no.5, 052008 (2023) doi:10.1103/PhysRevD.107.052008 [arXiv:2206.07501 [hep-ex]].
- [22] A. Datta, D. Marfatia, and L. Mukherjee, " $B \rightarrow K \nu \nu$ ", MiniBooNE and muon g-2 anomalies from a dark sector," Phys. Rev. D 109, no.3, L031701 (2024) doi:10.1103/PhysRevD.109.L031701 [arXiv:2310.15136 [hep-ph]].
- [23] A. Datta, J. L. Feng, S. Kamali, and J. Kumar, "Resolving the $(g-2)_{\mu}$ and \hat{B} Ånomalies with Leptoquarks and a Dark Higgs Boson," Phys. Rev. D **101**, no.3, 035010 (2020) doi:10.1103/PhysRevD.101.035010 [arXiv:1908.08625 [hep-ph]].
- [24] J. Liu, N. McGinnis, C. E. M. Wagner, and X. P. Wang, "A light scalar explanation of $(g-2)_{\mu}$ and the KOTO anomaly," JHEP **04**, 197 (2020) doi:10.1007/JHEP04(2020)197 [arXiv:2001.06522 [hep-ph]].
- [25] B. Batell, N. Lange, D. McKeen, M. Pospelov, and A. Ritz, "Muon anomalous magnetic moment through the leptonic Higgs portal," Phys. Rev. D 95, no.7, 075003 (2017) doi:10.1103/PhysRevD.95.075003 [arXiv:1606.04943 [hep-ph]].
- [26] A. Datta, S. Kamali, and D. Marfatia, "Dark sector origin of the KOTO and MiniBooNE anomalies," Phys. Lett. B 807, 135579 (2020) doi:10.1016/j.physletb.2020.135579 [arXiv:2005.08920 [hep-ph]].
- [27] D. P. Aguillard et al. [Muon g-2], "Measurement of the Positive Muon Anomalous Magnetic Moment to 0.20 ppm," Phys. Rev. Lett. 131, no.16, 161802 (2023) doi:10.1103/PhysRevLett.131.161802 [arXiv:2308.06230 [hep-ex]].